Shahrood University of Technology

Journal of Mining and Environment (JME)

Journal homepage: www.jme.shahroodut.ac.ir

Iranian Society of Mining Engineering (IRSME)

Numerical Simulation of Grout Penetration in Rock Fractures Considering Time-Dependent Viscosity and Density Effects in Saline and Fresh Water Systems

Alireza Sadooghi [1], Ali Aalianvari[2,1*], and Hamidreza Shahbazian[3]

1. Department of Mining Engineering, University of Kashan, Kashan, Iran
2. Department of Mining and Environmental Engineering, Faculty of Engineering, Tarbiat Modares University, Tehran, Iran
3. Department of Mechanical Engineering, University of Kashan, Kashan, Iran

Article Info

Received 11 October 2025
Received in Revised form 2 November 2025
Accepted 19 November 2025
Published online 19 November 2025

DOI: 10.22044/jme.2025.16963.3336

Keywords

Time-dependent viscosity
Penetration length
Grout
Saline water

Abstract

The study investigated how time-dependent viscosity affects the penetration length of cement-based grouts prepared with saline and fresh water. An idealized horizontal fracture, represented by two smooth, parallel, and frictionless plates, was assumed. The grout viscosity, varying over time, was analyzed to determine the maximum penetration length under a constant injection period. A fracture model was developed and meshed in Gambit, and the two-phase fluid behavior with time-dependent viscosity was simulated in ANSYS Fluent. One saline water function and two fresh water functions were examined. The saline grout was tested at 1475 and 1625 kg/m³, while the fresh water grouts were analyzed at 1475 kg/m³. The resulting penetration lengths were 1.384 m and 1.789 m for the fresh water grouts, and 0.789 m and 0.427 m for the saline grouts, respectively. The outcomes reveal that saline water grout penetrates less effectively than fresh water grout. Furthermore, the effect of density was found to be minor compared to viscosity variations, though differences between saline and fresh water systems were clearly evident. This study introduces a stable grout formulation without additives, contrasting with previous research that relied on additives and adjustments to the water-to-cement ratio, which led to grout instability over time. Utilizing CFD simulations, this research models a two-phase water-cement mixture with varying densities and viscosities, treated as a non-Newtonian fluid. Furthermore, the viscosity of the grout over time under hydraulic pressure is examined, providing valuable insights into grout behavior under subsurface conditions.

1. Introduction

As the demand for underground infrastructure increases, water leakage in critical structures such as dams, tunnels, and reservoirs presents significant challenges. Stabilized grout, composed of cement, water, and various additives, has emerged as an effective solution for reinforcing and sealing vulnerable areas, particularly under high-pressure conditions. The success of grout injection is heavily influenced by its rheological properties, especially the time-dependent variations in viscosity, which directly affect grout flow dynamics and penetration. Grouting operations consist of multiple stages, with the final extrusion stage being particularly crucial for ensuring optimal sealing and preventing future leakage. A thorough understanding of time-dependent viscosity is essential for the effective placement of grout, especially when dealing with varying hydraulic and environmental conditions. In conclusion, a comprehensive approach to grouting design—incorporating viscosity, density, and time-dependent behavior—is vital for optimizing the performance of underground systems, thereby supporting the sustainable development of infrastructure in an era of increasing demand for subterranean construction [1].

Corresponding author: ali_aalianvari@modares.ac.ir (A. Aalianvari)

Viscosity is a key factor in grout performance, affecting flow, penetration, and substrate interaction. It gradually increases during preparation and then sharply rises during injection, impacting the grout's ability to seal fractures. The water-to-cement (w/c) ratio significantly influences viscosity; low ratios result in high viscosity and poor flow, while high ratios create a fluid grout that cannot penetrate fractures effectively. Optimizing the w/c ratio is essential for balancing penetration and bonding. Understanding both initial and time-dependent viscosity is critical for effective grout design. Li et al.'s models provide valuable insights for improving grouting systems, considering geomechanical conditions and project-specific needs [2]. Advanced rheological models, such as the Herschel-Bulkley model, effectively describe the time-dependent viscosity behavior of cement-based grouts, capturing their non-Newtonian characteristics influenced by shear stress and cement hydration. Integrating these models into computational fluid dynamics (CFD) tools, including ANSYS Fluent and COMSOL Multiphysics, significantly enhances the accuracy and predictive capabilities of grouting simulations. These models improve the estimation of injection pressures, grout dispersion, and sealing efficiency, thereby supporting the optimization of grouting designs and enhancing the effectiveness of underground sealing operations [3]. Simulation studies conducted by Yi et al. and Yang et al. led to the formulation of robust theoretical models based on distinct flow structures, from which precise analytical expressions were derived to estimate key parameters such as propagation range, injection pressure, and penetration depth during grouting operations [4, 5]. Building on the concept of time-dependent viscosity, Rona et al. introduced a pioneering analytical model that comprehensively describes grout transport dynamics in fractured rock masses, significantly advancing the understanding of grout movement in complex and heterogeneous geological environments [6]. Incorporating time-dependent viscosity into these models improves the accuracy of predictions for key injection parameters and grout behavior. Additionally, Asad developed a real-time framework that accounts for viscosity variations, enhancing water displacement predictions and optimizing grouting operations, particularly in fractured and complex geological formations where traditional models may fall short [7]. Cement-based grouts, like rheopectic fluids, exhibit an increase in viscosity under shear stress, which significantly impacts their flow characteristics and sealing efficiency. The viscosity and rheological properties of grout are critical in determining its behavior, particularly under time-dependent stress-strain conditions. Accurate modeling is essential to optimize grout performance in complex geological and engineering environments [8, 9]. Sonbi's study explored the viscosity behavior of cement-based grouts, providing insights into their complex rheological properties. Related research assessed diutan gum and welan gum with fly ash as viscosity modifiers, showing their ability to enhance grout stability and flow. Additionally, Shahmaran et al. examined the impact of natural zeolite on time-dependent viscosity, highlighting its role in improving grout injection efficiency and sealing performance, especially in fractured environments [10]. To gain a deeper understanding of the underlying mechanisms, subsequent studies have extensively investigated the influence of time-dependent viscosity on grout transport dynamics. Yi et al. introduced highly refined analytical formulations that precisely describe grout flow behavior behind tunnel shield walls, providing a crucial framework for predicting grout distribution in confined and dynamically variable underground environments [4]. Building on this foundational work, Li et al. conducted precise measurements of apparent viscosities across a range of mixture ratios, developing comprehensive time-dependent models that accurately capture the evolving rheological properties of cementitious grouts under both static and dynamic conditions [11]. Further advancing these methodologies, Asad introduced an innovative real-time framework for the simultaneous assessment of water displacement driven by viscosity variations, enabling dynamic monitoring of grout behavior throughout the injection process. This groundbreaking approach significantly enhances the precision of grout placement, optimizing sealing efficiency and flow control in complex, fractured rock masses, where traditional models often fall short [7].

Experimental studies have shown that in grouts with time-dependent viscosity, the injected volume decreases, and uneven distribution occurs, leading to incomplete sealing. This presents significant challenges, particularly in applications where uniform fracture filling is required to maintain long-term structural integrity and hydraulic isolation. Accurate predictive models are crucial for optimizing grout placement, managing viscosity fluctuations, and ensuring effective fracture filling in complex subterranean environments [12]. Grout penetration, influenced

by factors such as injection pressure, viscosity, and fracture geometry, is critical for grouting operations. Adjusting the water-to-cement ratio effectively controls penetration, thereby impacting injection efficiency, structural reinforcement, and project costs. Excessive leakage or insufficient penetration can result in material loss and reduced effectiveness, highlighting the importance of optimizing grout rheology and injection parameters to improve efficiency and ensure long-term stability [13, 14].

Accurately capturing grout behavior remains challenging due to the inherent sensitivity of laboratory experiments to testing conditions. Under high stress, grout tends to accumulate in areas with high stress concentration, such as large fractures and high-friction pathways, which enhances penetration in these localized regions. Additionally, groundwater flow has been shown to significantly affect grout migration, underscoring the importance of incorporating hydrogeological conditions into grout modeling to achieve more accurate predictions [15]. Zhao et al. further demonstrated that an increase in yield stress substantially reduces grout penetration length, while irregular joint apertures can significantly alter grout propagation behavior, emphasizing the pivotal role of fracture geometry and mechanical properties in determining grout flow dynamics [16]. In a subsequent study, Rafi and Steel proposed an analytical framework to define stopping criteria, offering a systematic approach to control grout propagation and ensure that the grout reaches a predetermined penetration distance. This method significantly contributes to optimizing grouting practices, particularly in applications where precise grout placement is essential for effective structural reinforcement [17]. Experimental data indicate that grout viscosity increases exponentially as it sets, necessitating dynamic adjustments to the injection parameters. Higher injection rates are recommended during the low-viscosity phase, while, as viscosity increases, it becomes critical to reduce the injection rate and increase pressure to maintain continuous grout flow and prevent blockages. Saeedi et al. developed a numerical model to estimate grout volume and penetration, accounting for the influence of rock mass properties on grout injection behavior. This model serves as a comprehensive predictive tool for evaluating grout performance in heterogeneous geological conditions, providing valuable insights into grout distribution and aiding in the optimization of grouting operations [18]. Until the 1990s, stopping criteria for grouting operations were predominantly empirical. However, subsequent theoretical advancements resulted in the development of more precise, quantitatively grounded criteria, based on key parameters such as the minimum grout flow rate and the maximum achievable injection pressure [13, 19–20]. Notable contributions from Hassler et al., Lombardi, and Mohajerani et al. emphasized the importance of penetration length as a key indicator of grouting effectiveness, as it directly correlates with the extent of reinforcement achieved within fractured rock masses and significantly influences long-term structural stability [13, 21–22]. Building upon this understanding, Steel et al. introduced the concept of real-time injection control, a novel stopping criterion based on the continuous observation of grout propagation dynamics during the injection process [23]. This innovative approach facilitates adaptive adjustments to the injection parameters, thereby optimizing grout distribution and ensuring more efficient sealing. Furthermore, it has been demonstrated that increasing the water-to-cement (w/c) ratio enhances grout spread, leading to a longer penetration distance. Time-dependent viscosity experiments corroborate the ability to control grout behavior effectively by adjusting the mix ratio. Higher-viscosity grouts, characterized by their thicker consistency, exhibit a smaller effective radius and are more suited for sealing wide fractures, while lower-viscosity grouts, which spread more easily, are ideal for filling narrow cracks or fractures.

In relation to the innovation of this study, it is important to highlight that previous research has not employed a stable grout formulation without additives. Instead, prior studies relied primarily on laboratory experiments involving the addition of additives and adjustments to water-to-cement ratios, without taking into account other influencing factors for immediate setting times. This approach led to significant shortcomings. The grout formulations used in earlier methods gradually lost their durability, stability, and setting properties over time, revealing deficiencies that ultimately led to operational challenges.

In contrast, this study represents the first attempt to conduct simulations and sensitivity analysis using Computational Fluid Dynamics (CFD) software, specifically focusing on a two-phase water-cement mixture with varying densities and viscosity functions. This mixture was modeled as a non-Newtonian rheopectic fluid and utilized as a stable base grout. A major innovation of this research was the investigation of the viscosity

behavior of this two-phase fluid over time under the defined conditions using CFD software, resulting in substantial and satisfactory outcomes. Another key innovation of this study was the assessment of grout viscosity over time under hydraulic pressure conditions for grout injection. The hydraulic pressure applied during the experiments was consistent with the sub-headwater pressure and the pressure exerted on subsurface structures. To enhance the understanding of the subject and the steps involved in solving the problem using the software, the methodology employed in this research is presented as a classified algorithm (Figure 1).

Table 1. Definitions and Descriptions Provided by the Authors Regarding Time-Dependent Viscosity, Grout Penetration Length in Fractures, and the Composition of Stable Grout

Authors	Definitions and Descriptions Provided by the Authors Regarding Time-Dependent Viscosity, Grout Penetration Length in Fractures, and the Composition of Stable Grout
(Fang et al., 20252019; Zhang et al., 2025) [24,25]	The maximum grout penetration length is influenced by injection pressure, viscosity, and environmental conditions. Optimal design, achieved through gradual pressure control, can enhance penetration and mitigate potential hydraulic issues.
(Zhu et al., 2024) [14]	Innovative Experiments on Improving Grout Penetration Using Oscillatory Techniques.
(Mu et al., 2024) [26]	The viscosity of the grout is time-dependent, and the injection pressure affects the fracture diaphragm. Contrary to the assumption of the surrounding rock being rigid, its variability must be taken into account when analyzing the injection process.
(Wang et al., 2025) [27]	An increase in the water-to-cement ratio results in a reduction of compressive strength and an extension of the grout setting time, which consequently diminishes its effectiveness and penetration capability within the fracture and fissure network of the rock.
(Zhang, 2025) [28]	The accurate selection of the water-to-cement ratio and additives, combined with the control of the physical and chemical properties of the grout, plays a crucial role in enhancing viscosity, permeability, and the overall success of reinforcement and sealing projects.
(Khoshzaher, E, et al., 2025) [32]	The paper investigates how using fiber-reinforced shotcrete in tunnel construction affects ground settlement. Through a case study of the Tabriz metro line 2, the research demonstrates that this material effectively reduces ground settlement compared to conventional shotcrete.
(Barri, F et al., 2024)[6]	This study analyzes how the properties of soil and grout mixtures influence ground surface settlement during mechanized tunnel excavation. The research concludes that optimizing the grout mixture composition is a key factor in controlling and minimizing settlement.
(Chakeri, H et al., 2023)[14]	This research experimentally investigates how adding steel fibers to concrete improves the mechanical properties of segments used in tunnel lining. The study finds that steel fiber reinforcement enhances the strength and durability of the linings, making them more effective for mechanized tunneling.

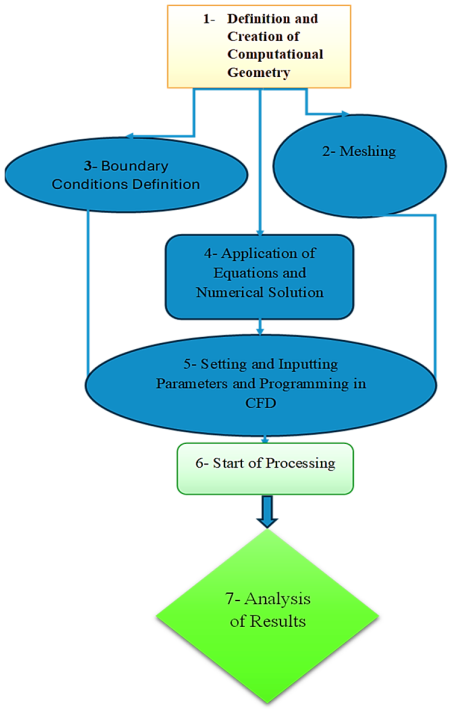

Figure 1. Solution algorithm, methodology, and research steps.

As shown in the figure, the general process of the research and simulation in the software consists of the following stages:

1. Definition and creation of the computational geometry for the system under consideration.
2. Mesh generation.
3. Boundary condition definition, including the specification of surface conditions and slurry injection under hydraulic pressure.
4. Application of equations and numerical analysis using the relevant governing equations.
5. Setting and inputting parameters involves specifying physical properties such as density, viscosity, surface tension, hydraulic pressure, and other necessary numerical inputs programmed into the CFD software.
6. Initiating processing through the software.
7. Analysis of the results.

1.1 . Fundamental assumptions and modeling prerequisites

Successful grout injection necessitates a comprehensive analysis and sophisticated modeling of fluid behavior within fractures and fissures. In this context, a set of essential assumptions and modeling prerequisites is formulated, each aimed at ensuring an accurate simulation of the grout injection process and fluid flow within fractured rock environments.

1. The fracture is assumed to be smooth, horizontal, and frictionless.
2. Given that the grout flow within the fracture is laminar (not turbulent) and no significant interaction exists between the upper and lower contact surfaces, the effect of gravity on the grout is neglected.
3. The pressure is assumed to be constant along the entire length of the fracture.
4. The rock wall surface is considered impermeable, preventing water from the grout from penetrating the rock walls.

1.2. Model Development Prerequisites and Flow Equations

Successful grout injection necessitates a thorough examination of fluid dynamics within fractures and fissures, supported by advanced modeling techniques that precisely replicate grout behavior in fractured rock environments. To achieve this, a set of fundamental assumptions and modeling prerequisites is carefully established, each designed to simulate the grout injection process and its fluid flow characteristics with high accuracy, ensuring a realistic representation of subsurface conditions.

The modeling of fluid flow is based on Darcy's law for radial flow in porous and fractured media, which serves as a comprehensive framework for determining key parameters such as flow rate (injection discharge), injection pressure, permeability, and fracture stability during the injection process. These models are particularly effective in analyzing grout behavior in radial fractures and calculating grout penetration into fractures over time, thereby providing valuable insights into grout distribution and its performance under varying injection conditions.

A critical factor in the injection process is the hydrodynamic velocity (or injection rate), which plays a decisive role in determining the success of the injection. If the injection rate exceeds a certain threshold, the suspended cement particles within the grout may fail to fully penetrate the fractures, leading to incomplete fracture coverage and potentially resulting in an ineffective injection. Consequently, both injection rate and pressure must be carefully regulated to prevent these issues, ensuring that grout placement and penetration are optimized for maximum effectiveness.

The radial flow equation is employed to calculate the flow rate toward or away from a borehole in a porous medium, establishing a clear relationship between grout penetration length and injection time. As expressed in (Equation 1) [32–35], this equation serves as a fundamental tool for predicting grout behavior, enabling engineers to refine and optimize grouting operations for enhanced efficiency and effectiveness.

$$qt=2\Pi a(r_t^2-r_a^2) \quad (1)$$

Where are:

q - is the flow rate or injection rate in liters per minute

t - is time in seconds for the transient state

a - is the diaphragm width or cross-sectional area of flow in square millimeters

which in the radial case is (2π)

r_t - is the grout penetration length in meters

and r_a - is the radius of the injection fracture in millimeters.

The injection borehole is significantly smaller in diameter compared to the overall grout propagation area, requiring precise modeling to effectively account for the disparity in scale between the borehole and the extensive fracture network that the grout must infiltrate. The total injection time is defined as the period from the initiation to the completion of grout injection, encompassing the entire grout movement process. The "start of grout" is specifically defined as the moment when grout begins to flow and enters the fracture network, marking the commencement of the injection process. This phase continues until the grout reaches its yield stress, at which point the flow properties of the grout undergo a transition, driven by changes in its rheological characteristics as the grout sets.

1.3. Viscosity Functions Used in the Time-Dependent Model

To investigate the variation of grout fluid viscosity, different viscosity functions are employed. The viscosity functions used for simulation and processing include the following:

μ_1 = exp (-29.92835+0.59485 t -0.00236 t^2) FOR 1475 DENSITY

μ_2 = exp (-47.93616+1.03133 t -0.00477 t^2) FOR 1475 DENSITY

μ_3 = exp (162.19485+6.84442 t -0.02162 t^2+ 0.0000387585 t^3-0.0000000248518 t^4) FOR 1475, 1625

Density

It is essential to highlight that the viscosity functions employed are based on scientific literature pertaining to the viscosity of both saline and fresh water. Furthermore, the density values, which represent the water-to-cement ratio at varying mix proportions, have been randomly selected across a range of values. This approach aims to investigate the effects of these parameters on the stoppage time of the grout, while simultaneously assessing the influence of time-dependent viscosity. The interplay between these factors is carefully examined to understand their combined impact on grout behavior over time.

1.4. Investigation of fluid flow type

To model fluid dynamics in fractures and determine the optimal approach in ANSYS Fluent, it is crucial to assess the flow regime (laminar or turbulent) using the Reynolds number. This dimensionless number compares inertial forces to viscous forces. If the Reynolds number is less than 2300, the flow is laminar; between 2300 and 4000, it is transitional; and if it exceeds 4000, the flow is turbulent. The Reynolds number helps identify the flow regime, facilitating accurate simulations of fluid behavior in fractures and geotechnical applications [29-32].

$$RE=\frac{\rho VD}{\mu} \quad (2)$$

In this expression Where are:

P - denotes the density of water ($g\cdot cm^{-3}$)

V - is the fluid velocity ($m\cdot s^{-1}$)

D - is the pipe diameter (mm)

μ - is the dynamic viscosity of the fluid expressed in poise ($g\cdot cm^{-1}\cdot s^{-1}$).

If the Reynolds number exceeds 4000, the flow is regarded as turbulent. Thereafter, the Reynolds number is calculated for each fluid mixture according to the corresponding relation (Table 2).

Table 2. Calculated Reynolds number for each fluid mixture according to the corresponding relation

RE_{1-10}	Reynolds number
$RE_1=\frac{\rho VD}{\mu}=\frac{1475*0.0015589303*1}{46.9196}$	0.048
$RE_2=\frac{\rho VD}{\mu}=\frac{1475*3.6864549*1}{29.39114}$	184.91
$RE_3=\frac{\rho VD}{\mu}=\frac{1475*0.000091094121*1}{169.0166639067}$	0.079
$RE_4=\frac{\rho VD}{\mu}=\frac{1625*0.000096023722*1}{169.0166639067}$	0.092

A comprehensive analysis of the Reynolds numbers, derived from viscosity calculations under various conditions-including different densities and both two-dimensional configurations-unequivocally confirmed that the flow regime remains laminar in all scenarios. This definitive conclusion firmly supports the classification of the flow regime as laminar, thereby necessitating the precise definition of corresponding simulation parameters within the software, meticulously tailored to reflect the laminar flow characteristics with the highest degree of accuracy.

2. Methodology and Case Study

2.1. Simulation, Geometry Construction, and Computational Mesh Generation:

The primary aspect of the problem must be thoroughly addressed to establish a robust foundation for the modeling process. To ensure a rigorous, methodical, and systematic analysis, the following steps should be executed in a precise and sequential manner:

1. Define and construct the final model within the simulation software, ensuring a comprehensive understanding of the modeling objectives and the underlying physical principles governing the system.

2. Create the geometry and generate the computational mesh with meticulous attention to detail, ensuring that the mesh has sufficient resolution and accuracy to represent the geometrical complexity of the fracture system and borehole structure.
3. Select the appropriate solver and physical model, ensuring that the solver chosen aligns with the expected physical phenomena—such as fluid flow, heat transfer, and fracture interaction—and accurately reflects the subsurface conditions and grout behavior.
4. Perform the necessary computational simulations and generate visual representations of the results to validate the model's predictive accuracy and evaluate the performance of the grouting process in real-world conditions.
5. Iteratively refine the model parameters—both numerical and physical—based on preliminary results, optimizing the model to improve its accuracy and realism, thereby capturing dynamics that may not have been fully considered in the initial model.

Step two necessitates the use of advanced software capable of both geometry creation and mesh generation with high precision. CAD systems or specialized ANSYS products are typically suitable for this purpose, provided they offer comprehensive drafting capabilities and ensure seamless compatibility with simulation tools. In this study, Gambit software was employed to construct the model and generate the computational mesh, which was subsequently used for detailed computational fluid dynamics (CFD) analysis.

Initially, a model that replicates real-world conditions with high fidelity is constructed to simulate fluid movement through fractured rock. As illustrated in the following sections, the model incorporates a drilled borehole intersected by pre-existing fractures, accurately simulating grout injection into these fractures. The grout is introduced at the injection inlet and propagates through the subsurface fractures, mimicking the real-world behavior of grout during the injection process. A comprehensive model of the borehole, fractures, injection inlet, and grout flow paths is developed to capture the full scope of the injection process. This model serves as the core framework within the software, facilitating an in-depth analysis of grout penetration and the dynamic interactions between fluid flow and fracture geometry.

Figure 2 illustrates a detailed representation of the initial model of the borehole and its associated fractures, meticulously incorporating the surrounding rock mass and non-rigid walls. The model is constructed using the advanced capabilities of ANSYS Fluent, providing a comprehensive framework for simulating the grout injection process.

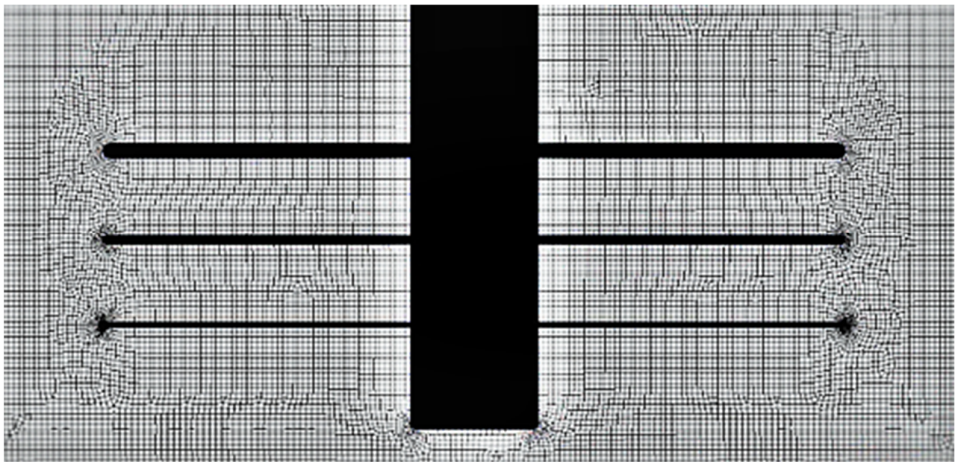

Figure 2. Schematic of 2D meshing for simulating a symmetric cavity in a concrete dam wall in Ansys Fluent.

As illustrated in the figure above, the fracture network and its surrounding rock mass are meticulously modeled to closely replicate real-world geological conditions. This approach is integral to the study's objective of simulating near-realistic field scenarios, where the intricate interactions between the injected grout and the surrounding geological matrix are of paramount importance. To achieve the highest level of accuracy in this simulation, the fracture walls are represented as elastically deformable structures. This representation enables a precise depiction of their dynamic response to a range of factors, including pressure fluctuations, grout injection

rates, and mechanical interactions with the surrounding rock mass. The flexibility of the fracture walls is crucial for capturing the non-linear, stress-dependent behaviors of fractured rock under applied pressures, which can vary significantly during the grout injection process.

By incorporating such advanced modeling techniques, this study provides an unprecedented level of detail in understanding fluid-rock interactions during grout injection. This approach ensures that the simulation captures the full spectrum of factors affecting grout behavior, from the initial injection phase to the stabilization of the system. This enhanced level of detail is essential for developing reliable predictive models that can inform real-world applications in geotechnical engineering, tunnel construction, and other subsurface operations.

2.2. Boundary Conditions and Problem Assumptions

Defining the boundary conditions of a model is a fundamental and indispensable step in the model development process. The approach used to establish these boundary conditions significantly influences the accuracy and reliability of fluid flow simulations. This section presents the boundary conditions and a set of initial assumptions for the model that has been developed.

For the initial model setup, a fracture with a length of 8 meters, an inlet diameter of 2 mm, and an outlet diameter of 1 mm is defined. This two-dimensional (2D) model is created in Gambit to simulate the fluid flow dynamics within the fracture (Figure 3). The model incorporates the fracture inlet, outlet, upper and lower fracture walls, and a meshed region within the fracture itself. In this preliminary configuration, both the inlet and outlet are left open to enable the assessment of the maximum grout penetration length and to validate the simulation's performance. The surrounding fracture walls are assumed to be impermeable, ensuring that fluid flow is confined to the fracture path. Additionally, the injection pressure along the borehole is disregarded for simplification purposes, corresponding to the entire length of the fracture. It is essential to emphasize that the model dimensions and boundary conditions were optimized through an iterative trial-and-error process, specifically tailored for simulating laminar fluid flow. This is particularly relevant given that the flow of slurry within fractures is predominantly laminar in nature under typical conditions. Moreover, the model assumes homogeneous viscosity and density across all scenarios, aligning with the core focus of the study, which investigates the primary objective of the research. The precision in defining these parameters is critical for ensuring the reliability and validity of the simulation results within the context of the study's objectives.

The fracture aperture is non-uniform along its length, gradually narrowing toward the outlet, thereby simulating more realistic fracture conditions. Specifically, the aperture decreases as the distance from the fracture inlet increases, which mirrors the behavior observed in natural fractures during fluid injection processes. A pressure differential of 0.01 bar is applied across the fracture, with the pressure increasing incrementally from the inlet to the outlet. This pressure gradient is critical for understanding the evolving flow dynamics within the fracture, and it plays a vital role in influencing the grout's behavior as it propagates through the fracture network. Moreover, the fracture terminus is left open to facilitate the examination of grout stop time along the fracture length, offering valuable insights into the flow dynamics and the eventual stabilization of the grout within the fracture system.

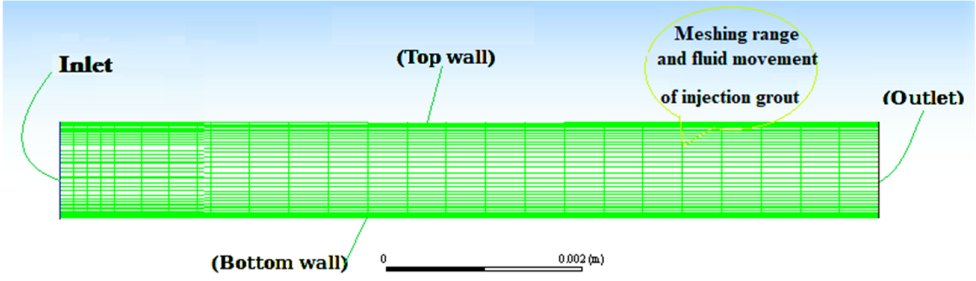

Figure 3. Boundary conditions and parameter specifications in the 2D model.

One of the principal innovations of this study is the advanced simulation of a two-phase fluid system. In this simulation, water is initially defined as the primary fluid phase, with a constant density

of 1000 g/cm³, while a slurry is used as the secondary (injected) fluid phase, characterized by varying densities of 1475 g/cm³ and 1625 g/cm³. This dual-phase modeling approach is indispensable for accurately capturing the complex interactions and flow dynamics of multi-phase fluid systems, particularly in geotechnical and subsurface applications.

In the context of ANSYS Fluent, a crucial prerequisite for initiating a two-phase fluid simulation is the precise definition of the constituent phases. Each phase must be distinctly defined to ensure the software can accurately recognize and simulate their interactions. This step is essential for constructing a coherent two-phase fluid mixture within the computational model. The accurate specification of the properties of each phase—such as density, viscosity, and phase behavior—is fundamental for capturing the full range of interactions that occur in two-phase flow, especially when simulating complex materials like slurry mixtures.

3. Results and Discussion

Figure 4 provides a comprehensive visualization of the initial simulation of fluid movement within the borehole, conducted using ANSYS Fluent. As depicted in the figure, the slurry is injected from the upper part of the borehole and begins to flow along its primary flow path within the cavity. It gradually infiltrates into the connected fractures on both the left and right sides.

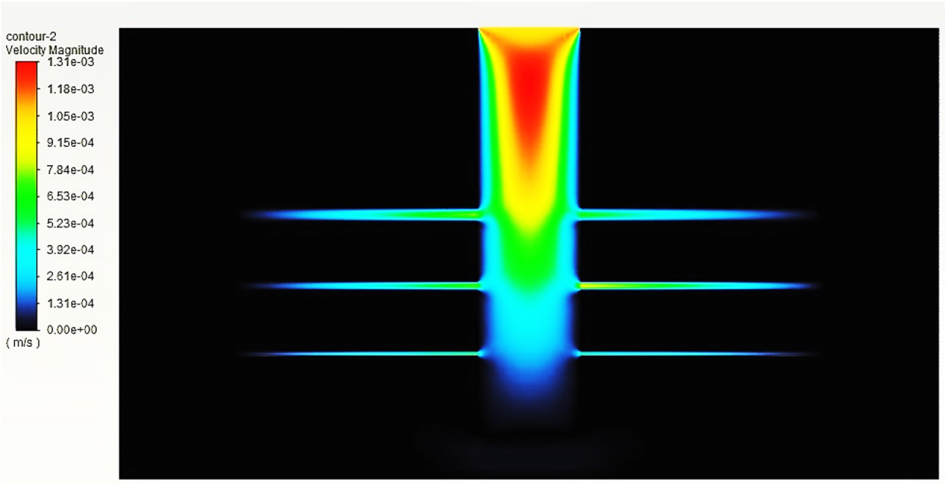

Figure 4. Fluid movement in the borehole and its penetration into the existing fractures and cracks.

Upon completion of the processing steps, the slurry reached its final stopping point as both viscosity and concentration increased progressively. The definitive position of the fluid within the fracture was accurately recorded. As shown in the figure below, the deceleration of the fluid within the fracture, as it approaches a stationary state, is clearly demonstrated (Figure 5). Moreover, due to the intrinsic geometric characteristics of the fracture, a notable variation in slurry velocity was observed between the fracture walls and the central axis, resulting in a distinct phase separation. This two-phase separation is distinctly illustrated in Figure 5, providing a clear and comprehensive visual representation of the fluid dynamics involved.

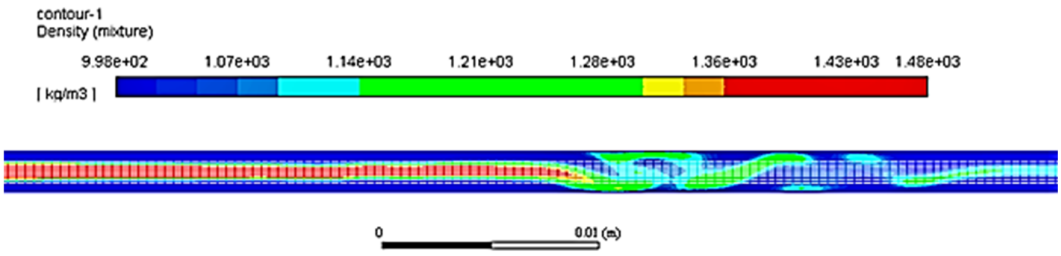

Figure 5. Fluid stopping location in the fracture with variations in fluid viscosity and density.

Subsequently, all numerical results and output data, derived from the post-processing and meticulous analysis of both two-dimensional and three-dimensional fluid simulation models across all combined scenarios, are presented in Table 3 below. The table offers a thorough and exhaustive analysis of key parameters, including viscosity, stopping location, processing time, and fluid density, across a range of cement-water combinations, thereby providing profound insights into the complex fluid dynamics involved.

Table 3. Data from post-processing and analysis of the simulation models.

Functions	Fluid viscosity ($kg \cdot m^{-1} \cdot s^{-1}$)	Penetration length (m)	Actual fluid processing time (min)	Fluid density ($kg \cdot m^{-3}$)	Composition of various water-to-cement ratios
μ_1	46.91	1.384	11	1475	1:1
μ_2	29.39	1.789	11	1475	1:1
μ_3	169.01	0.789	11	1475	1:1
μ_4	169.01	0.427	11	1625	0.7:1

As shown in Table 1, various viscosity functions, derived from preliminary data and analysis, are provided alongside the results obtained from processing and modeling the slurry fluid behavior in fractures. These outputs, which include the fluid's stopping position (in meters) at a fixed time of 11 minutes, are presented for different fluid densities and varying water-to-cement ratios. Therefore, the subsequent section will focus on a detailed analysis and discussion of the results derived from these output data.

3.1. Overall Results Analysis

The figure below presents a comparative analysis of two distinct viscosity functions for freshwater with a density of 1475 kg/m³ and a processing duration of 11 minutes (Figure 6). The horizontal axis represents the viscosity function, while the vertical axis corresponds to the fluid penetration length, measured in meters. The blue dashed curve illustrates the relationship between fluid viscosity and penetration depth within the fracture. These curves depict the penetration lengths for two distinct viscosity functions: the first viscosity function and the second viscosity function. The red markers, varying in size, indicate the stopping positions for each viscosity function, with marker size being directly proportional to the penetration length; larger markers correspond to deeper penetration. The first viscosity function results in a penetration length of 1.384 meters over the 11-minute processing period, while the second viscosity function reaches a penetration length of 1.789 meters during the same time frame, indicating superior penetration. This demonstrates a clear, direct relationship between viscosity and fluid penetration behavior. The second viscosity function, characterized by its specific rheological properties, facilitates enhanced penetration within the fixed processing time.

Upon examining the influence of viscosity on penetration length, it becomes evident that the fluid governed by the higher viscosity of the second function penetrated further than the fluid governed by the first function. This outcome can be attributed to the distinct rheological properties and increased viscosity of the second fluid, which, under specific conditions, promote enhanced penetration. These results are consistent with empirical observations of non-Newtonian fluid behavior and the dynamics of two-phase fluid systems, underscoring the critical role of viscosity in governing fluid movement and penetration within fractured media.

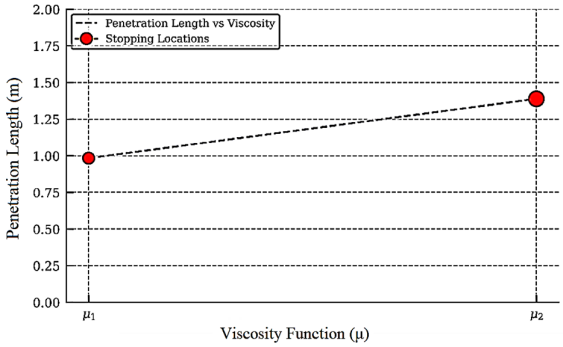

Figure 6. Comparison of penetration length for two fresh-water viscosity functions at the same density and processing time.

The figure below presents a comparative analysis of fluid penetration for saline water at two different densities (1475 kg/m³ and 1625 kg/m³) over a fixed processing time of 11 minutes (Figure 7). The horizontal axis represents the viscosity function, while the vertical axis shows the fluid penetration length in meters. The blue dashed curve illustrates the relationship between viscosity and

penetration depth within the fracture. These curves represent the penetration behavior of the fluid under two distinct viscosity functions: the first viscosity function and the second viscosity function. Red markers, varying in size, indicate the stopping positions for each viscosity function, with marker size being directly proportional to the penetration length; larger markers correspond to greater penetration.

At a density of 1475 kg/m³, the fluid achieves a penetration length of 0.789 meters. However, when the density increases to 1625 kg/m³, the penetration length decreases to 0.427 meters. This results in an absolute reduction of 0.362 meters, which represents a relative decrease of approximately 45.9%. This substantial reduction underscores the significant inhibitory effect of increased density on fluid penetration, even when the processing time and rheological function remain constant.

The observed reduction can primarily be attributed to the dominant role of density in limiting fluid movement within the fracture. This effect is particularly pronounced in cases involving saline water flowing through horizontal fractures with smooth, frictionless surfaces, where, in the absence of friction, density and viscosity become the primary controlling factors. Additionally, the change in the water-to-cement ratio—from 1:1 to 0.7:1, as indicated in the table—occurred concurrently with the increase in density. A lower water-to-cement ratio typically results in increased viscosity, which further reduces penetration. While some of the observed difference in penetration length can be attributed to this ratio change, the predominant influence is clearly due to the variation in density.

For engineering applications, such as rock mass consolidation and flow control in hydraulic structures, these findings highlight the crucial importance of controlling slurry density. When the objective is to maximize penetration within a fixed time frame, lower-density saline water is more effective. Conversely, if the aim is to restrict penetration and control the injection front, increasing the slurry density can be an efficient strategy. Specifically, increasing the density from 1475 to 1625 kg/m³ resulted in a reduction in penetration from 0.789 meters to 0.427 meters, representing a 45.9% decrease in penetration length.

In conclusion, under the examined conditions, the effect of density dominates over variations in the viscosity function and should be considered a critical design parameter for slurry injection operations. These results align with established theoretical principles in fluid mechanics governing non-Newtonian fluids and two-phase systems within fractured media, providing valuable insights for optimizing slurry injection processes in practical engineering applications.

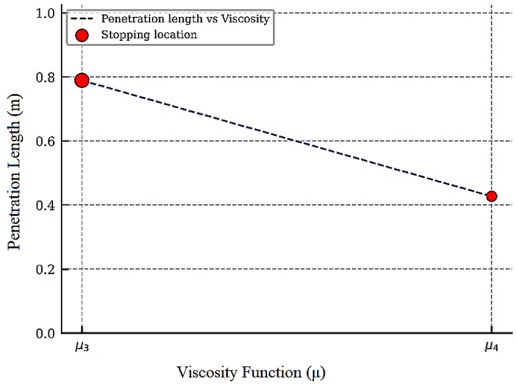

Figure 7. Penetration length in saline water at two densities (1475 and 1625 kg/m³) after 11 minutes.

The figure below provides a comparative analysis of fluid penetration lengths for two different fluids (fresh water and saline water) at comparable densities, under a fixed processing time of 11 minutes. The horizontal axis represents the viscosity function, while the vertical axis shows the fluid penetration length, measured in meters (Figure 8). This chart illustrates how the viscosity and density of fresh water and saline water slurries influence their penetration lengths in fractures. The data is highly relevant to geotechnical engineering, civil engineering, and slurry injection operations within fractured media.

The results indicate the following penetration lengths for the two fluids at different densities and a fixed processing time:

1. The first viscosity function of fresh water, with a density of 1475 kg/m³, yields a penetration length of 1.384 meters.
2. The second viscosity function of fresh water, with a density of 1475 kg/m³, results in a penetration length of 1.789 meters.
3. The third viscosity function of saline water, with a density of 1475 kg/m³, achieves a penetration length of 0.789 meters.
4. The fourth viscosity function of saline water, with a density of 1625 kg/m³, results in a penetration length of 0.427 meters.

These results clearly demonstrate that fresh water penetrates further than saline water, and that an increase in the density of saline water significantly reduces its penetration length.

3.2. Effect of Density and Viscosity on Penetration Length

Fresh water, characterized by lower viscosity, exhibits greater penetration length. In contrast, saline water, which has higher viscosity and greater density, encounters more resistance to flow, thus demonstrating reduced penetration depth.

For fresh water with a density of 1475 kg/m³, the penetration length is 1.384 meters, whereas saline water at the same density only achieves 0.789 meters of penetration. When the density of saline water increases to 1625 kg/m³, its penetration length further decreases to 0.427 meters. This reduction can be attributed to the combined effects of increased hydrostatic pressure and viscous resistance, both of which hinder the fluid's motion.

The data conclusively show that fresh water with a density of 1475 kg/m³ penetrates significantly further than saline water at the same density (1.384 meters compared to 0.789 meters). Moreover, increasing the density of saline water to 1625 kg/m³ results in a further reduction in penetration length to 0.427 meters, representing a 45.9% decrease.

These trends indicate that both density and viscosity play a critical role in controlling fluid penetration depth within fractured media. When higher-density saline water is used, its increased viscosity and hydrostatic forces limit fluid movement, leading to reduced penetration. On the other hand, fresh water, with lower density and viscosity, allows for greater penetration, making it more effective for applications where maximal fluid infiltration is required.

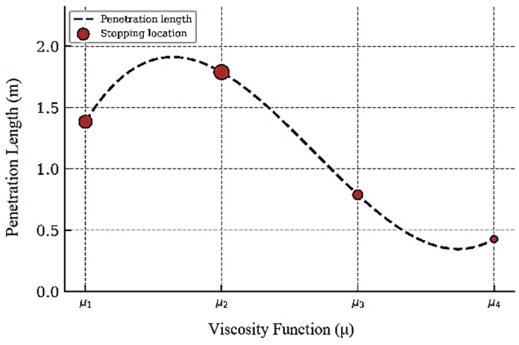

Figure 8. Comparison of penetration length for two different functions (fresh water and saline water).

The figure below illustrates the relationship between slurry density and fluid penetration length in a saline water system, analyzed across different densities and under a fixed processing time of 11 minutes. The horizontal axis represents slurry density in kg/m³, while the vertical axis denotes fluid penetration length in meters (Figure 9). The data points are presented as red circles, each corresponding to the measured penetration lengths for various saline water densities. To enhance the visual clarity and accuracy of the data, a blue dashed curve has been interpolated, representing a continuous and smoothed relationship between density and penetration length.

The chart clearly demonstrates an inverse correlation between slurry density and penetration length. Specifically, as slurry density increases from 1475 kg/m³ to 1625 kg/m³, the penetration length decreases from 0.789 meters to 0.427 meters, all under the fixed processing time of 11 minutes. This reduction in penetration length underscores the significant impact of slurry density on the fluid's ability to advance through fractures and narrow pathways within the substrate.

Key Findings

1. Fresh water with a density of 1475 kg/m³ exhibits greater penetration than saline water at the same density, highlighting the influence of fluid type on penetration behavior.
2. An increase in the density of saline water leads to a substantial decrease in penetration length, emphasizing the dominant role of density in fluid flow within fractures.

The figure below presents a detailed analysis of the relationship between viscosity and penetration length in a two-phase fluid system. On the horizontal axis, viscosity is represented in Pascal-seconds, while the vertical axis corresponds to fluid penetration length, measured in meters (Figure 10). This chart clearly illustrates an inverse relationship between viscosity and penetration length: as viscosity increases, the penetration length decreases.

The inverse relationship between viscosity and penetration length is strongly evidenced by the plotted data. As viscosity increases, the fluid's ability to penetrate the medium is substantially diminished. The red data points (small circles) represent the experimentally measured viscosity and penetration lengths under specific conditions. To provide a smoother and more continuous representation of the data, a blue dashed curve has been interpolated. This curve enhances the clarity of the visualization, offering a more refined interpretation of the relationship between viscosity and penetration.

The chart unequivocally demonstrates that as viscosity increases, the penetration length

decreases in a progressive manner. This inverse correlation is significant for fluid dynamics, particularly in fractured or porous media, where fluid movement must be precisely controlled.

Key Insights:

1. A strong inverse relationship exists between viscosity and penetration length, with higher viscosity fluids exhibiting markedly reduced penetration into the medium.
2. The interpolated blue dashed curve provides a more refined and continuous depiction of the relationship, enhancing the accuracy of the data representation.

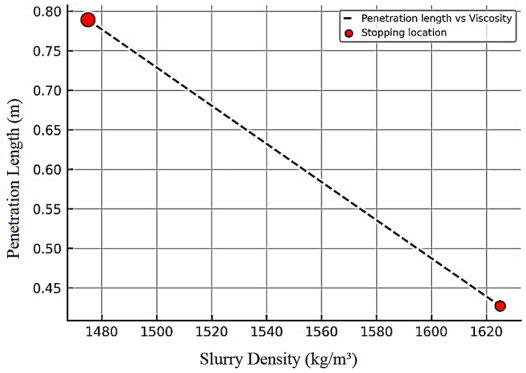

Figure 9. Inverse relation between density and penetration length in saline water at 11 minutes of injection.

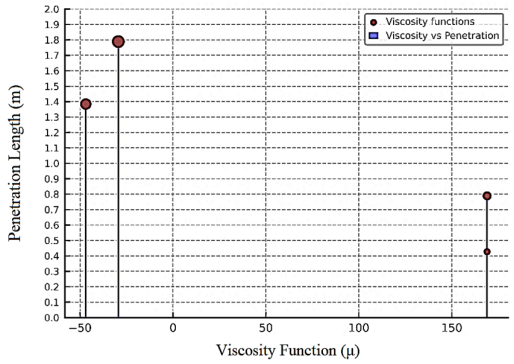

Figure 10. Relationship between viscosity and penetration length in a two-phase system.

This study thoroughly investigates the effects of viscosity and density on the penetration length of slurries within horizontal fractures. The simulations and modeling conducted provide valuable insights into the behavior of two-phase fluids across a range of environments, significantly advancing our understanding of fluid dynamics in confined systems.

3.3. Influence of Viscosity on Fluid Penetration Length

The simulation results conclusively demonstrate that viscosity has a direct, significant impact on fluid penetration length. Specifically, as viscosity increases, penetration length decreases. This outcome can be attributed to the increased resistance to flow that high-viscosity fluids experience in confined spaces, such as horizontal fractures. While high-viscosity fluids may exhibit greater ease of movement in open, low-resistance systems, the confined nature of horizontal fractures significantly impedes their ability to advance. This resistance results in a reduced penetration depth, which is a critical consideration in many geotechnical and hydraulic applications.

3.4. Influence of Density on Fluid Penetration

In addition to viscosity, this study also explored the impact of fluid density on penetration length. The results clearly indicate that as the density of the fluid increases, the penetration length decreases. Denser fluids, owing to their greater mass, exhibit distinct dynamics compared to less dense fluids. These fluids experience higher hydrostatic pressure and greater resistance to flow, which reduces their ability to penetrate the medium. This effect is particularly evident in systems involving saline and freshwater, where variations in fluid density are a key determinant in fluid behavior.

3.5. Interaction of Viscosity and Density

Notably, the findings suggest that the effect of viscosity on penetration length is more pronounced than that of density. Although density does influence penetration depth, it has a lesser effect compared to viscosity. For instance, saline water with a higher density exhibited reduced penetration over a fixed period, relative to freshwater. However, viscosity remains the dominant factor controlling fluid penetration. This observation indicates that, in certain fluid systems, density variations may have a relatively minor influence on penetration, especially when compared to the more significant effect of viscosity.

3.6. Confirmation of Simulation Results

The simulation results further substantiate the conclusion that both viscosity and density significantly affect fluid penetration within horizontal fractures. Fluids with higher viscosity and greater density consistently exhibited shorter penetration lengths, confirming the role of

increased resistance to flow in limiting penetration. These findings align with existing research on two-phase fluid behavior, which indicates that both viscosity and density are critical factors in determining how effectively a fluid can infiltrate fractured media.

3.7. Density vs. Viscosity: A Comparative Analysis

An interesting aspect of the study is the relative impact of viscosity and density on penetration length. While density variations across different fluids, particularly between saline and freshwater, influence penetration depth, the effect of viscosity was generally more pronounced. This suggests that viscosity plays a more significant role in fluid behavior under controlled conditions, with density acting as a secondary, though still important, factor in determining penetration depth. Despite this, variations in fluid density between freshwater and saline water were distinguishable, with each demonstrating distinct impacts on penetration behavior.

4. Conclusions

This study offers a comprehensive and in-depth examination of the effects of viscosity and density on the penetration length of slurries within horizontal fractures. By utilizing simulations and advanced modeling techniques, the study significantly contributes to the understanding of two-phase fluid behavior, providing essential insights into the fluid dynamics within fractured media. Additionally, this study innovatively employs a stable grout formulation without additives, contrasting with previous research that relied on additives and water-to-cement ratio adjustments. Prior methods led to grout instability over time. The study employs CFD simulations to analyze a two-phase water-cement mixture with varying densities and viscosities, modeled as a non-Newtonian fluid. It also evaluates grout viscosity under hydraulic pressure, offering key insights into grout behavior in subsurface conditions. The key findings from the simulations and analytical results are as follows:

Viscosity as the Principal Determinant of Penetration: The study establishes a clear, inverse relationship between fluid viscosity and penetration length. As viscosity increases, the fluid's ability to penetrate the fracture medium diminishes substantially due to increased resistance to flow within confined spaces. This insight is crucial for optimizing fluid injection processes, especially in geotechnical and hydraulic engineering applications where controlling the fluid's movement is vital for achieving effective results.

The findings demonstrate that an increase in fluid density leads to a decrease in penetration length. Denser fluids experience greater hydrostatic pressure and higher resistance to flow, thus restricting their capacity to infiltrate fractured media. While the effect of density is significant, it is secondary to the effect of viscosity. Viscosity remains the dominant factor influencing fluid movement and, consequently, penetration depth. The study also reveals the interplay between viscosity and density in governing fluid penetration. While both factors play a role, viscosity exerts a more substantial influence on penetration depth than density. Although variations in density—especially between saline and fresh water—affect penetration behavior, viscosity proves to be the more critical determinant in controlling fluid movement. This highlights the importance of prioritizing viscosity management in the design and optimization of fluid injection systems.

This research offers valuable insights into fluid-driven processes, particularly for slurry injection, subsurface fluid transport, and hydraulic fracturing. The study emphasizes the importance of controlling viscosity and density to optimize fluid penetration and enhance system performance in industries such as dam construction, tunneling, and chemical processing. A thorough understanding of how viscosity, density, and penetration length interact is crucial for managing fluid flow in fractured media, especially in complex subsurface environments. By adjusting these parameters, fluid penetration can be optimized, improving efficiency and performance across various engineering applications. The findings not only reinforce principles of fluid mechanics but also provide a foundation for future advancements in slurry injection and fluid transport systems.

Statements and Declarations

The authors declare that they have no conflict of interest.

Competing Interests

This research work is not supported by any funding agency.

Financial Disclosure Statement

The author(s) received no specific funding for this work.

Funding

This research did not receive any specific grants from funding agencies in the public, commercial, or not-for-profit sectors.

Data Availability

The data presented in this study are available on request from the corresponding author

Consent for Publication

All the authors have read and agreed to the submitted version of the manuscript

References

[1]. Hao, Y., et al. (2023). Application of polymer split grouting technology in earthen dam: Diffusion law and applicability. *Construction and Building Materials, 2023. 369: p. 130612.* 10.1016/j.conbuildmat.130612

[2]. Lee, J., et al.(2000) Numerical and experimental analysis of penetration grouting in jointed rock masses. *International Journal of Rock Mechanics and Mining Sciences, 37(7): p. 1027–1037.* 10.1016/S1365-1609(00)00040-X

[3]. Inazumi, S., K. Tazuke, and S. Kashima. (2025). Time-Dependent Rheological Behavior and MPS Simulation of Cement–Bentonite Slurries with Hydration Accelerators for Borehole Backfilling Applications. J*ournal of Composites Science, 9(7): p. 361. 10.3390/jcs9070361*

[4]. Ye, F., et al.(2013), Back-filled grouts diffusion model of shield tunnel considering its viscosity degeneration. Zhongguo Gonglu Xuebao *(China Journal of Highway and Transport), 26(1): p. 127–134.* 10.3969/j.issn.1001-7372.2013.01.017

[5]. Yang, Z., et al.(2015), *Study on diffusion parameters of Bingham fluid based on column-hemispherical penetration grouting. J. Sichuan Univ, **47**: p. 47–53.* 10.3969/j.issn.1000-5024.2015.01.008

[6]. Barri, F., Chakeri, H., Darbor, M., Haghkish, H. (2024). The effect of soil and grout mixture on the ground surface settlement in mechanized excavation, *Journal of Mining and Environment, 15(4), 1607-1626*

[7]. Assaad, J.J.(2015), Correlating water extraction to viscosity variations of injection grouts. C*onstruction and Building Materials, 77: p. 74–82.* 10.1016/j.conbuildmat.2014.12.024

[8]. Bird, R.B., R.C. Armstrong, and O. Hassager,(1987) Dynamics of polymeric liquids. *Vol. 1: Fluid mechanics.* 10.1002/pol.1978.130160210

[9]. Eklund, D. and H. Stille,(2008) Penetrability due to filtration tendency of cement-based grouts. T*unnelling and Underground Space Technology,. 23(4): p. 389–398.* 10.1016/j.tust.2007.06.011

[10]. Şahmaran, M., et al., Evaluation of natural zeolite as a viscosity-modifying agent for cement-based grouts. *Cement and Concrete Research, 38(7): p. 930–937.* 10.1016/j.cemconres.2008.03.007

[11]. Li, S., et al.(2013), Research on time-dependent behavior of viscosity of fast curing grouts in underground construction grouting. *Chinese Journal of Rock Mechanics and Engineering, 32(1): p. 1–7.* 10.3969/j.issn.1000-6915.2013.01.001

[12]. Nazari, M. H., Aalianvari, A., & Tani, M. E. (2025). Contrary trends of grout consumption and water absorption at Sardasht. *Scientific Reports, 15(1), 4667.*

[13]. Hassler, L., H. Stille, and U. Hakansson. (2023). Simulation of grouting in jointed rock. *in Isrm Congress. ISRM.*

[14]. Chakeri, H., Darbor, M., Sh. Maleki, F., Minaee, T. (2023). Experimental investigation of steel fibers' effect on the improvement of mechanical properties of concrete segmental lining in mechanized tunneling, *Rudarsko-geološko-naftni zbornik, 38(3), 55-63*

[15]. Zou, L., U. Håkansson, and V. Cvetkovic,(2018). *T*wo-phase cement grout propagation in homogeneous water-saturated rock fractures. *International Journal of Rock Mechanics and Mining Sciences, 106: p. 243–249.*

10.1016/j.ijrmms.2018.04.017

[16]. Eftekhari, A., Aalianvari, A., & Rostami, J. (2018). Influence of TBM operational parameters on optimized penetration rate in schistose rocks, a case study: Golab tunnel Lot-1, Iran. *Computers and Concrete, An International Journal, 22(2), 239-248. DOI: https://doi.org/10.12989/cac.2018.22.2.239*

[17]. Rafi, J. and H. Stille,(2021). A method for determining grouting pressure and stop criteria to control grout spread distance and fracture dilation. *Tunnelling and Underground Space Technology, 112: p. 103885.* 10.1016/j.tust.2021.103885

[18]. Saeidi, O., H. Stille, and S.R. Torabi,(2013). Numerical and analytical analyses of the effects of different joint and grout properties on the rock mass groutability. *Tunnelling and Underground Space Technology, 2013. 38: p. 11–25.* 10.1016/j.tust.2013.01.001

[19]. Jahanmirir, Shirin, Ali Aalianvari, and Hossein Ebrahimpour-Komleh.(2024). "Optimizing groundwater seepage prediction in tunnels using the human mental search (HMS) algorithm: a cognitive-inspired approach to complex geotechnical challenges." *Journal of Mining and Environment* .

[20]. Nazari, M. H., Uromeie, A., & Aalianvari, A. (2023). Coupled grout flow: Fracture deformation effects on grout penetration in a physical model. *Iranian Journal of Science, 47(3), 765-777. 10.1016/S0886-7798(01)00004-9*

[21]. Lombardi, G.(2003)., Grouting of rock masses, in Grouting and ground treatment. *p. 164–197.*

[22]. Mohajerani, S., et al.(2015), *G*rout penetration in fractured rock mass using a new developed explicit algorithm. *international journal of Rock Mechanics and Mining Sciences, 80: p. 412–417.* 10.1016/j.ijrmms.2015.06.013

[23]. Stille, B., et al.(2009)., Experience with the real time grouting control method. *Geomechanics and Tunnelling, 2(5): p. 447–459.* 10.1002/geot.200900036

[24]. Fang, K., Zhao, T., Tan, Y., & Qiu, Y. (2019). Prediction of grouting penetration height along the shaft of base grouted pile. *Journal of Marine Science and Engineering, 7(7), 212.* 10.3390/jmse7070212

[25]. Zhang, S., Åberg, W., Johansson, F., Funehag, J., & Zou, L. (2025). Experimental Study on Erosion and Viscous Fingering of Fresh Cement-Based Grout After Injection Stops. *Rock Mechanics and Rock Engineering, 1–18.*

[26]. Mu, W., Li, L., Liu, H., Ren, B., Chen, J., & Wang, X. (2024). An experimental study on fracturing response and slurry flow of high-pressure grouting in fractured rock. *Rock Mechanics and Rock Engineering, 57(7), 4533–4558.* 10.1007/s00603-024-02645-9

[27]. Wang, K., Chen, P., Xu, K., Yang, C., Li, Y., & Zong, H. (2025). A forchheimer-based fluid-solid coupling model for nonlinear flow of power-law grouts in fractured rock grouting. *Scientific Reports*, *15(1), 29445.* 10.1038/s41598-025-25973-9

[28]. Zhang, S. (2025). Cement-based grouting of rock foundations for new and existing dams *KTH Royal Institute of Technology.*

[29]. Houlsby, A.C., (1991). Construction and design of cement grouting: a guide to grouting in rock foundations. *1991: John Wiley & Sons.*

[30]. Creager, M. and P.C. Paris,(1967). Elastic field equations for blunt cracks with reference to stress corrosion cracking. *International journal of fracture mechanics, 1967. 3(4): p. 247–252.* 10.1007/BF00017324

[31]. Bear, J(2013)., Dynamics of fluids in porous media. 2013: Courier Corporation.

[32]. Khoshzaher, E., Miri Darmarani, Sh., Chakeri, H., Darbor, M., Haghkish, H. (2025). The influence of fiber-reinforced shotcrete on the ground settlement in tunnel excavation: A case study of Tabriz metro line 2, *International Journal of Mining and Geo-Engineering, 59(1), 21-29 .2*

نشریه مهندسی معدن و محیط زیست
نشانی نشریه: www.jme.shahroodut.ac.ir
انجمن مهندسی معدن ایران
دانشگاه صنعتی شاهرود

شبیه‌سازی عددی نفوذ دوغاب در شکستگی‌های سنگی با در نظر گرفتن اثرات ویسکوزیته و چگالی وابسته به زمان در محیط‌های حاوی آب شور و آب شیرین

علیرضا صدوقی[1]، علی عالی‌انوری[2,1*] و حمیدرضا شهبازیان[3]

۱. گروه مهندسی معدن، دانشگاه کاشان، کاشان، ایران
۲. گروه مهندسی معدن و محیط زیست، دانشکده فنی و مهندسی، دانشگاه تربیت مدرس، تهران، ایران
۳. گروه مهندسی مکانیک، دانشگاه کاشان، کاشان، ایران

اطلاعات مقاله

تاریخ ارسال: ۲۰۲۵/۱۰/۱۱
تاریخ داوری: ۲۰۲۵/۱۱/۰۲
تاریخ پذیرش: ۲۰۲۵/۱۱/۱۹

DOI: 10.22044/jme.2025.16963.3336

کلمات کلیدی

گرانروی وابسته به زمان
طول نفوذ
دوغاب
آب شور

چکیده

این مطالعه بررسی کرد که چگونه ویسکوزیته وابسته به زمان بر طول نفوذ دوغاب‌های پایه سیمانی تهیه شده با آب شور و شیرین تأثیر می‌گذارد. یک شکستگی افقی ایده‌آل، که توسط دو صفحه صاف، موازی و بدون اصطکاک نشان داده می‌شود، فرض شد. ویسکوزیته دوغاب، که با گذشت زمان تغییر می‌کند، برای تعیین حداکثر طول نفوذ تحت یک دوره تزریق ثابت، تجزیه و تحلیل شد. یک مدل شکستگی در Gambit توسعه داده شد و شبکه‌بندی شد و رفتار سیال دو فازی با ویسکوزیته وابسته به زمان در ANSYS Fluent شبیه‌سازی شد. یک تابع آب شور و دو تابع آب شیرین بررسی شدند. دوغاب شور در غلظت‌های ۱۴۷۵ و ۱۶۲۵ کیلوگرم بر متر مکعب آزمایش شد، در حالی که دوغاب‌های آب شیرین در غلظت ۱۴۷۵ کیلوگرم بر متر مکعب تجزیه و تحلیل شدند. طول نفوذ حاصل به ترتیب ۱.۳۸۴ متر و ۱.۷۸۹ متر برای دوغاب‌های آب شیرین و ۰.۷۸۹ متر و ۰.۴۲۷ متر برای دوغاب‌های آب شور بود. نتایج نشان می‌دهد که دوغاب آب شور نسبت به دوغاب آب شیرین، نفوذ کمتری دارد. علاوه بر این، مشخص شد که اثر چگالی در مقایسه با تغییرات ویسکوزیته ناچیز است، اگرچه تفاوت‌ها بین سیستم‌های آب شور و شیرین به وضوح مشهود بود. این مطالعه یک فرمولاسیون دوغاب پایدار بدون افزودنی را معرفی می‌کند، برخلاف تحقیقات قبلی که بر افزودنی‌ها و تنظیمات نسبت آب به سیمان متکی بودند و منجر به ناپایداری دوغاب در طول زمان می‌شدند. این تحقیق با استفاده از شبیه‌سازی‌های CFD، یک مخلوط دو فازی آب-سیمان با چگالی‌ها و ویسکوزیته‌های متغیر را مدل‌سازی می‌کند که به عنوان یک سیال غیر نیوتنی در نظر گرفته می‌شود. علاوه بر این، ویسکوزیته دوغاب در طول زمان تحت فشار هیدرولیکی بررسی می‌شود و بینش‌های ارزشمندی در مورد رفتار دوغاب در شرایط زیرسطحی ارائه می‌دهد.

نویسنده مسئول مکاتبات: ali_aalianvari@modares.ac.ir (ع. عالی انوری)